We are IntechOpen,
the world's leading publisher of
Open Access books
Built by scientists, for scientists

4,800
Open access books available

122,000
International authors and editors

135M
Downloads

154
Countries delivered to

Our authors are among the

TOP 1%
most cited scientists

12.2%
Contributors from top 500 universities

CLARIVATE ANALYTICS

BOOK CITATION INDEX

INDEXED

WEB OF SCIENCE™

Selection of our books indexed in the Book Citation Index
in Web of Science™ Core Collection (BKCI)

Interested in publishing with us?
Contact book.department@intechopen.com

Numbers displayed above are based on latest data collected.
For more information visit www.intechopen.com

MEMS-Based Micro-heat Pipes

Qu Jian and Wang Qian

Additional information is available at the end of the chapter

Abstract

Micro-electro-mechanical systems (MEMS)-based micro-heat pipes, as a novel heat pipe technology, is considered as one of the most promising options for thermal control applications in microelectronic circuits packaging, concentrated solar cells, infrared detectors, micro-fuel cells, etc. The operating principles, heat transfer characteristics, and fabrication process of MEMS-based micro-grooved heat pipes are firstly introduced and the state-of-the-art of research both experimental and theoretical is thoroughly reviewed. Then, other emerging MEMS-based micro-heat pipes, such as micro-capillary pumped loop, micro-loop heat pipe, micro-oscillating heat pipe, and micro-vapor chamber are briefly reviewed as well. Finally, some promising and innovatory applications of the MEMS-based micro-heat pipes are reported. This chapter is expected to provide basic reference for future researches.

Keywords: micro-heat pipe, thermal control, capillary limitation, micro-cooler, MEMS

1. Introduction

Nowadays, the thermal management of electronics/optoelectronics remains to be a great challenge due to the continuous increasing heat flux to be dissipated with diminishing space associated with rapid advances in the microelectronic fabrication and packaging technology. Generally, the thermal control at the system level is not a serious problem since adequate conventional cooling schemes are available [1]. Cooling at the chip level that maintains both chip maximum temperature and temperature gradient at acceptable levels are in great demands. Many efforts have been made in the past two decades to develop novel micro-cooling technologies capable of removing larger amount of heat from chips [2–5], among which micro-heat pipes (MHPs) are considered as one of the most promising solutions.

MHPs, envisioned very small heat transfer components incorporated as an integral part of semiconductor devices as illustrated in **Figure 1**, have attracted considerable attention since they were first introduced by Cotter [6]. A MHP is also referred to micro-grooved heat pipe as depicted by Suman [7] and essentially has convex but cusped cross sections with dimension characteristics subject to the criterion given by Babin et al. [8]

$$\frac{r_c}{r_h} \geq 1 \tag{1}$$

where r_c and r_h are the capillary and hydraulic radius, respectively. Accordingly, the hydraulic radius of the total flow passage in a MHP is comparable in magnitude to the capillary radius of the vapor–liquid interface. This dimensionless expression better defines a MHP and helps to differentiate between small versions of conventional heat pipes and a veritable MHP. Typically, the cross-sectional dimensions of MHPs are in the range of 10–500 μm and lengths of up to several centimeters [9]. A MHP is so small that it does not necessitate additional wicking structures on the inner wall as used by conventional heat pipes to assist the return of condensate to the evaporator. Instead, the capillary forces are largely generated in the sharp edges of diverse small noncircular channel cross sections as illustrated in **Figure 2**, which serve as liquid arteries. The maximum heat flux dissipated using these micro-devices are reported to be as high as 60 W/cm^2 [11].
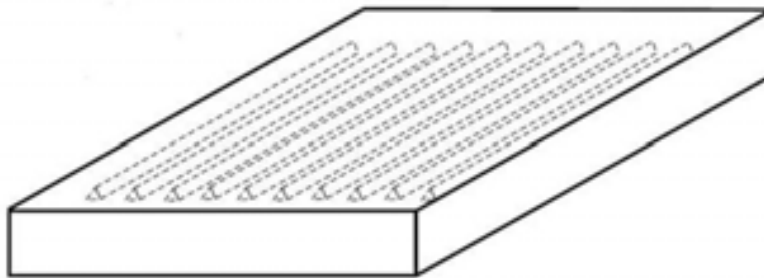

Figure 1. Micro-heat pipe array in silicon wafer.

Actually, MHPs are suitable for the direct heat removal from semiconductor devices because they could be fabricated and integrated into them, as envisioned by Cotter [6], on the basis of micro-electro-mechanical systems (MEMS) technology and work as thermal spreaders [12]. The advantages of MEMS-based MHPs mainly includes as follows: (1) It allows for precise temperature control at the chip level; (2) the overall cooling is more efficient because specific heat sources within the electronics package may be targeted and reduce the contact thermal resistance; (3) the overall size of the electronic system can be kept small and achieve material compatibility; and (4) easy to large scale replication and mass production. Due to the compact size, high local heat removal rates and can be used to effectively lower chip maximum temperature and attain temperature uniformity, MEMS-based MHPs could be considered as a promising option to meet future chip-level cooling demands.
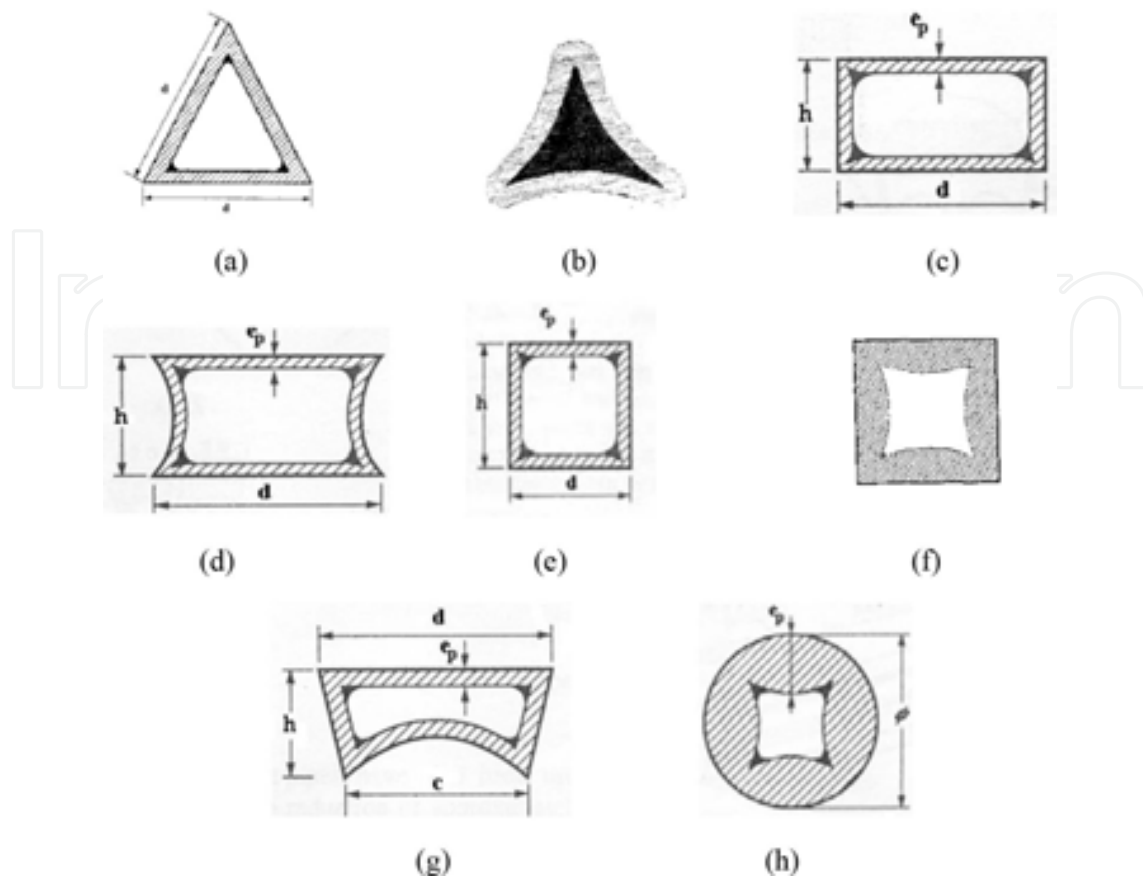
Figure 2. Cross-sections of individual micro-grooved heat pipes: (a, b) triangular section; (c, d) rectangular section; (e, f) square section; (g) trapezoidal section; (h) circular section [10].

For all practical situations, MHP is a general name for heat pipes with micro-wicks and mini-/micro-tubes in many references, and a heat pipe that satisfies the Bond number ($Bo = (\rho_l - \rho_g)g r_h^2 / \sigma$) to be on the order of 1 or less or capillary action dominates gravity can be termed as MHPs [7, 13]. The published reviews of MHPs were largely related to micro-grooved heat pipes [14–16], and there is no comprehensive introduction on MEMS-based MHPs. Moreover, the concept of MEMS-based MHPs, in this chapter, are not simply limited to micro-grooved heat pipes etched on silicon wafers but also other novel types that fabricated through MEMS technology. The overall size of a MEMS-based heat pipe device should be comparable to that of an electronic chip, regardless of having wicking structures or not.

In this chapter, we present a review on the MEMS-based MHPs that begin with a brief introduction of micro-grooved heat pipes, including working principles, heat transport limitations, and fabrication approach. The following section focuses on the state-of-the-art of research on MEMS-based micro-grooved heat pipes both experimentally and numerically, and then advances made in some other emerging MEMS-based MHPs. Meanwhile, some promising and potential applications of MEMS-based MHPs are also reported. It is expected to provide a basis for MEMS-based MHP design, performance improvement, and further expansion in its applications.

2. Micro-grooved heat pipe

2.1. Fundamental operating principles

The fundamental operating principles of micro-grooved heat pipes are essentially the same as those occurring in conventional heat pipes and can be easily understood by using a triangular cross section MHP as illustrated in **Figure 3**. Heat applied to one end of the MHP, called evaporator, vaporizes the liquid in that region and pushes the vapor toward the cold end, called condenser, where it condenses and gives up the latent heat of vaporization. In between the evaporator and the condenser is a heat transport section, called the adiabatic section, which may be omitted in some cases. MHPs do not contain any wicking structures, but consist of small non-circular channels and the role of wicks in conventional heat pipes gives way to the sharp-angled corner regions, serving as liquid arteries. The vaporization and condensation processes cause the curvature of liquid–vapor interface (see **Figure 3**) in the corner regions to change continually along the passage and result in a capillary pressure difference between the hot and cold ends. The capillary force generated from the corner regions pump the liquid back to the evaporator and the circulation of working fluid inside the MHP accompanied by phase change is then established [17, 18].
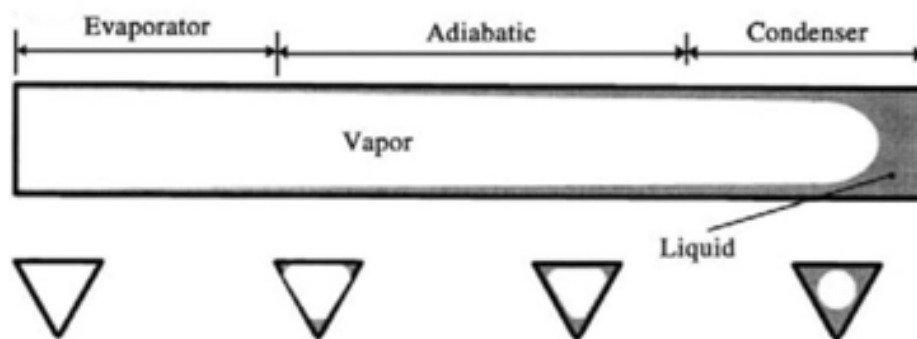

Figure 3. Schematic diagram of a micro-heat pipe with triangular cross-section.

2.2. Heat transport limitations

The operation and performance of heat pipes are dependent on many factors such as the tube size, shape, working fluid, and wicking structure. The maximum heat transport capability of a heat pipe operating at steady state is governed by a number of limiting factors, including the capillary, sonic, entrainment, and boiling limitations [18]. Theoretical and fundamental phenomena that cause each of these heat pipe limitations have been the subject of a number of investigations for conventional heat pipes. The representative work was given and discussed by many authors [19], while only a limited number concern the operating limitations in a MHP [20]. The experimental investigation by Kim and Peterson [21] revealed that the capillary limitation occurred before entrainment and boiling limitations. When the heat input is larger than a maximum allowable heat load, capillary limitation occurs and becomes the most commonly encountered limitation to the performance of a MHP [22, 23], which causes

the dry-out of the evaporator and degrades the thermal performance significantly. As a result, the capillary limitation is the primary concern of MHP design and operation according to its working principles. It can be concluded from the operating principles that the primary mechanism by which MHPs operates result from the difference in the capillary pressure across the liquid–vapor interfaces in the evaporator and condenser sections. For proper operation, the capillary pressure difference should be greater than the sum of all the pressure losses throughout the liquid and vapor flow passages. The gravity force is usually not taken into account in two-phase micro-devices compared to surface tension, and thus, the hydrostatic pressure drop can be neglected [24]. Hence, the relationship can be expressed mathematically as follows

$$\Delta p_c \geq \Delta p_l + \Delta p_v \tag{2}$$

where Δp_c is the net capillary difference, Δp_l and Δp_v are the viscous pressure drops in the liquid phase and vapor phase, respectively.

The left-hand side in Eq. (2) at a liquid–vapor interface can be estimated from Laplace-Young equation, and for most MHP applications it can be reduced to:

$$\Delta p_c = \sigma \left(\frac{1}{r_{ce}} - \frac{1}{r_{cc}} \right) \tag{3}$$

where r_{ce} and r_{cc} represent the minimum meniscus radius appearing in the evaporator and maximum meniscus radius in the condenser, respectively. Both values depend on the shape of the corner region and the amount of liquid charged to the heat pipe.

For steady-state operation with constant heat addition and removal, the viscous pressure drop occurring in liquid phase is determined by

$$\Delta p_l = \left(\frac{\mu_l}{K A_l h_{fg} \rho_l} \right) L_{eff} q \tag{4}$$

where L_{eff} is the effective heat pipe length defined as:

$$L_{eff} = 0.5 \left(L_e + L_c \right) + L_a \tag{5}$$

The viscous vapor pressure drop can be calculated similarly to the liquid vapor drop but is more complicated due to the mass addition and removal in the evaporator and condenser, respectively, as well as the compressibility of the vapor phase. Consequently, the dynamic

pressure should be included for a more accurate computation and thus elaborately analyzed by several researchers [17]. The resulting expression, for practical values of Reynolds number and Mach number, is similar to the liquid pressure drop and can be expressed as follows:

$$\Delta p_v = \left(\frac{C(f\,\mathrm{Re})_v \mu_v}{2 r_{h,v}^2 A_v h_{fg} \rho_v} \right) L_{eff} q \tag{6}$$

where $r_{h,v}$ is the hydraulic radius of the vapor space and C is a constant that depends on the Mach number [12, 25].

2.3. Fabrication process of MEMS-based micro-grooved heat pipes

In 1991, Peterson et al. [26] initialized the concept of using micro-grooved heat pipes as an integral part of the semiconductor devices. Normally, MEMS-based MHPs with hydraulic diameters on the order of 50–300 μm are directly etched into silicon wafers, and the directionally dependent wet etching or deep reactive ion etching (DRIE) processes are commercially available and widely utilized to create a series of parallel micro-grooves which shape the micro-devices [27–30]. The wet chemical etching process could create trapezoidal or triangular grooves, allowing etching of silicon wafers in one particular direction at a higher rate as compared to other directions, while DRIE process that uses physical plasma tool generates rectangular grooves. Once the micro-grooves are etched into the silicon wafer, a Pyrex 7740 glass cover plate is often bonded to the surface to form the closed channels based on anodic bonding technique for the visualization of two-phase flow in MHPs.

The lithographic masking techniques, coupled with an orientation-dependent etching technique, are typically utilized and Peterson [17] has summarized this processes. **Figure 4** gives an example of six major fabrication process with respect to a MEMS-based MHP having trapezoidal cross sections, including photolithography, wet etching, and anodic bonding. After standard clean and drying, a two-side polished (100) silicon wafer is thermally dry oxidized to form a layer of SiO$_2$, which is used as a hard mask for anisotropic wet etching as illustrated below. Firstly, one side of the silicon wafer is spun coated with a photoresist (PR) (**Figure 4a**). The patterned transfer from a mask onto the wafer is established via exposure and development (**Figure 4b**). Subsequently, buffered oxide etch (BOE) solutions are used to strip off the exposed SiO$_2$ (**Figure 4c**), and the remanent PR is removed by a cleaning step (**Figure 4d**). Then, some micro-grooves with trapezoidal cross sections are created by wet etching (**Figure 4e**). For flow visualization, a Pyrex 7740 glass is finally bonded with the silicon wafer after removing the SiO$_2$ layer using HF solution (**Figure 4f**). Before silicon-to-glass bonding, the laser drill technology is employed to create the inlet/outlet holes for evacuating and charging. After the completion of the MEMS fabrication process, the wafer is sliced into individual dice.
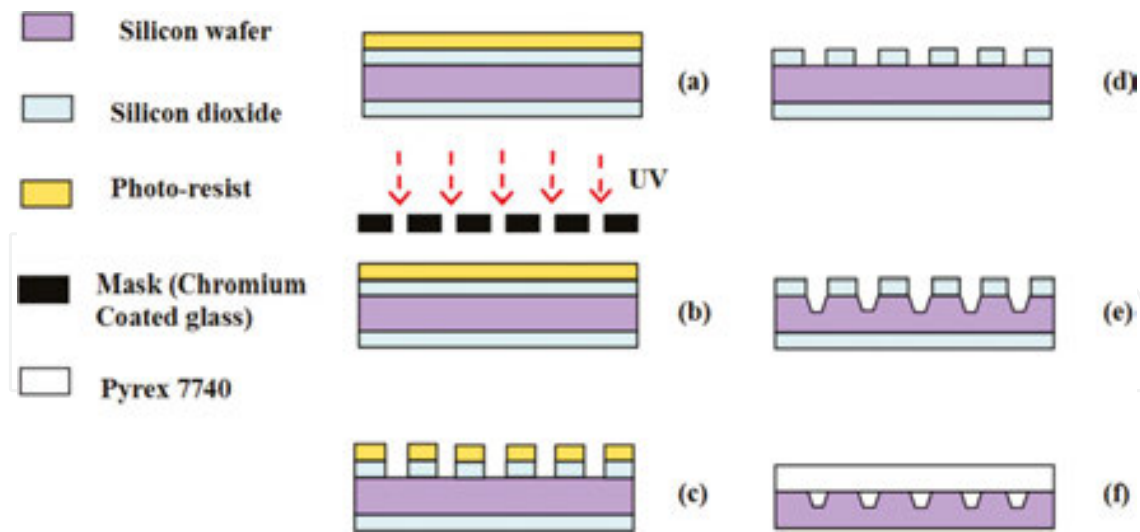
Figure 4. Fabrication processes of a MEMS-based MHP: (a) spin coating photoresist, (b) UV exposure, (c) BOE etching (d) wet etching, (e) HF etching silicon layer, and (f) silicon-to-glass anodic bonding.

In addition to the orientation-dependent etching processes, a more elaborate technique was developed that utilizes the multi-source vapor deposition process [31, 32] to create an array of long, narrow channels of triangular cross-section lined with a thin layer of copper. This process begins with the fabrication of a series of square or rectangular grooves in a silicon wafer. Then, the grooves are closed using a dual E-beam vapor deposition process, creating an array of long narrow channels of triangular cross section with two open ends. **Figure 5** gives a SEM image of the end view of a vapor deposited MHP which has not quite been completely closed at the top. Clearly, the MHPs are lined with a thin layer of copper, and thus the migration of the working fluid throughout the semiconductor material could be significantly reduced.

Figure 5. A vapor-deposited micro-grooved heat pipe [17].

3. State-of-the-art of research on MEMS-based micro-grooved heat pipes

3.1. Experimental investigation

The original conception of micro-grooved heat pipes fabricated in silicon substrate was first introduced by Cotter, but the first experimental test results on these micro-devices were not published until somewhat later by Peterson and coworkers [26]. In their investigation, several silicon wafers as shown in **Figure 6** were fabricated with distributed heat sources on one side and an array of MHPs on the other. As an intermediary step in the development process, experimental tests were conducted by Babin et al. [8] on two individual micro-grooved heat pipes, one copper and one silver, approximately 1 mm² in cross-section area and 57 mm in length. Distilled and deionized water were used as the working fluid.
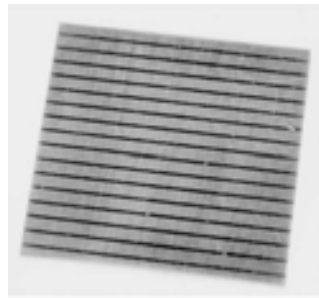
Figure 6. Array of micro-grooved heat pipes fabricated on silicon wafer [26].

After that, Peterson's group carried out several experimental and numerical investigations [28, 31, 33, 34] to verify the feasibility of MHPs as an integral part of semiconductor devices, and then a large number of experimental investigations have been conducted by other researchers to extend the MHP array concept and determine the potential advantages of MEMS-based MHPs.

In 1993, Peterson et al. [28] carried out the experiment on MHP arrays fabricated in silicon chips. As compared to a plain silicon wafer, their experiment demonstrated that the silicon chips of the same size integrated with rectangular and triangular MHP arrays charged with methanol could obtain reductions in the maximum temperature of 14.1 and 24.9°C, respectively, at a power input of 4 W. The effective thermal conductivities of these two MHP arrays were increased by 31 and 81%, respectively. Due to the higher capillary pumping effect, it is found that the thermal performance of a triangular MHP is better than that of a rectangular one. However, the experimental investigation by Badran et al. [35] shown an indistinctive increase in effective thermal conductivity after using MHP arrays fabricated on silicon substrate. Compared to plain silicon, the effective thermal conductivities were only increased by about 6 and 11% at high power levels using methanol and water as working fluids, respectively, which are far less than the predicted values based on a theoretical model. This result was found to be similar to the experimental results conducted by Berre et al. [36], according to whom that there was only a systematic slight temperature decrease in the charged MHP array of 55 parallel triangular-shaped channels for filling ratios between 6 and 66% as

compared with the empty MHP array at a heat input range between 0.5 and 4 W. However, this temperature discrepancy was found to be comparable to the experimental uncertainty and therefore no significant heat transfer enhancement could be clearly identified. These authors believed that it is mainly attributed to the large thermal conductivity of silicon, and therefore, a large part of heat is transferred by conduction through the silicon material and that the improvement due to the MHP array is negligible.

To enhance performance of MHPs, Kang and Huang [37] proposed two silicon MHPs with star and rhombus grooves, as illustrated in **Figures 7**a, b, respectively. The heat transfer performance of these MHPs was improved due to better capillarity provided by more acute angles and micro-gaps. Experimental results demonstrate that for the silicon wafer with an array of 31 star-grooved MHPs (340 μm in hydraulic diameter) filled with 60% methanol at a power input of 20 W, reduction in the maximum wafer temperature was 32°C. For the silicon wafer with an array of 31 rhombus-grooved MHP (55 μm in hydraulic diameter) filled with 80% methanol at a power input of 20 W, reduction in the maximum wafer temperature was 18°C. The best thermal conductivities of star and rhombus grooves MHPs were found to be 277.9 and 289.4 W/(m K), respectively.

Berre et al. [36] fabricated two sets of MHP arrays in silicon wafers. The first array, as illustrated in **Figure 8**a, was made from two silicon wafer with 55 triangular parallel micro-channels (230 μm in width and 170 μm in depth); and the second array, as illustrated in **Figure 8**b, was made from three silicon wafers having two sets of 25 parallel micro-channels, with the larger ones placed on the top of the smaller ones. The smaller triangular channels were used as arteries drain the liquid to the evaporator, so the liquid returns via independently etched channels to the evaporator rather than common liquid–vapor counter-current flow as occurred in **Figure 8**a, and thus significantly reducing the liquid–vapor interactions and enhancing the heat transport limitation. Ethanol and methanol were used as the working fluids. Filling ratios ranging from 0 to 66% were tested. The effective thermal conductivity evaluated by a 3D simulation was found to be 600 W/(m K), which represented an increase of 300% of the silicon thermal conductivity at high heat flux, demonstrating remarkable heat transfer enhancement.
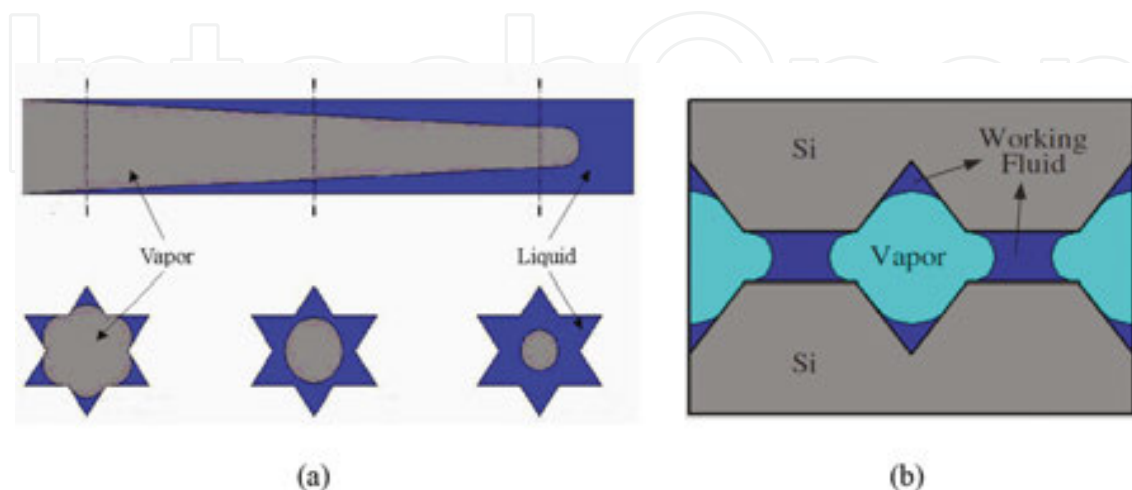

Figure 7. Schematic diagram of star grooves MHP (a) and rhombus grooves MHP (b) [37].
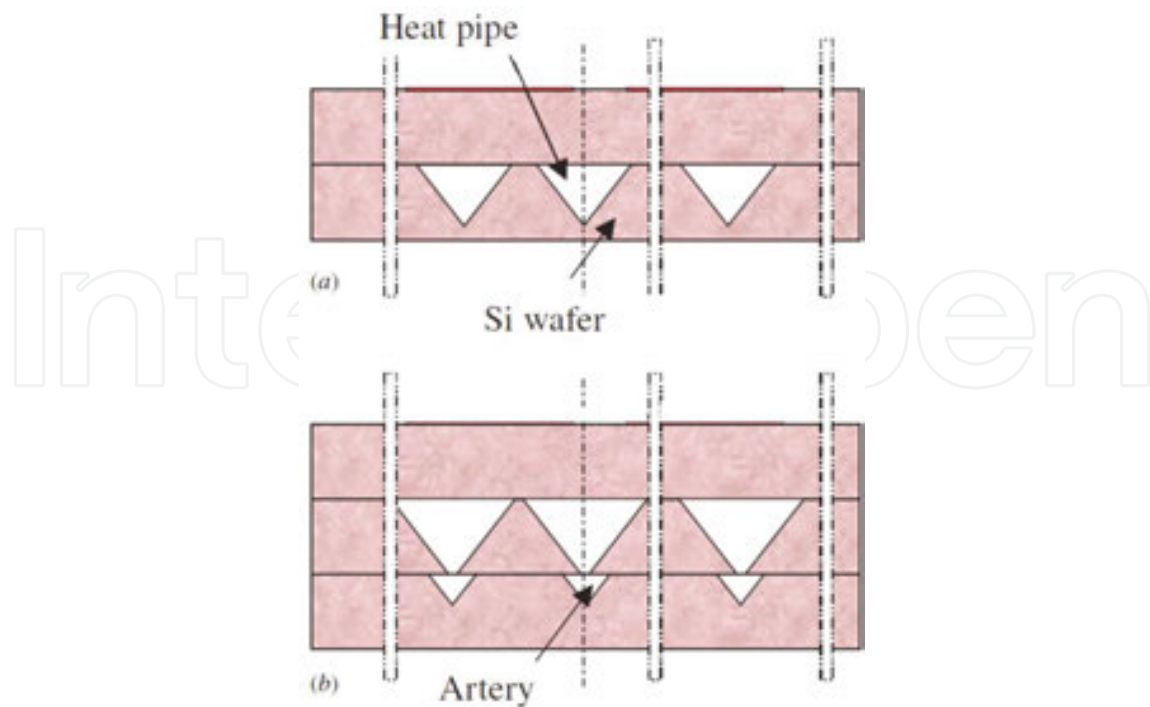
Figure 8. Transverse cross-sections of a MHP array (a) with triangular channels and (b) with triangular channels coupled with arteries [36].

Recently, a novel artery MHP array as illustrated in **Figure 9** was proposed by Kang et al. [38] to enhance the liquid backflow. Two smaller channels serving as arteries are positioned on both sides of one vein channel which acts as the ordinary MHP, and these channels are connected together at both ends by two connecting channels. Because of the two ends' pressure difference of the V-shape grooves in the MHP array, the working liquid gathered at the
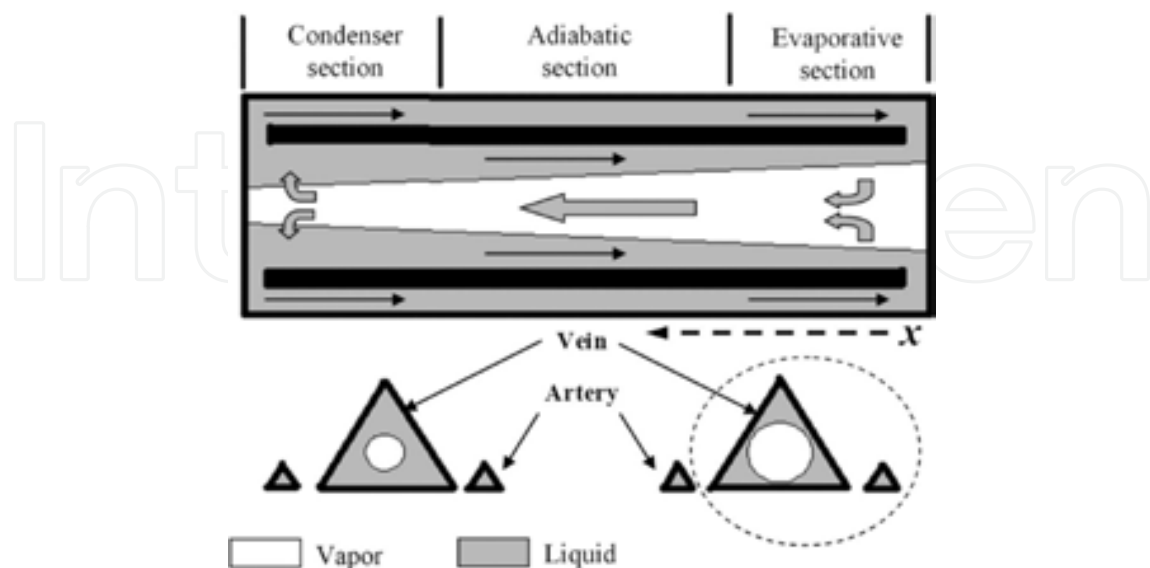

Figure 9. Schematic diagram of the MHP and artery and working principle [38].

condenser could be transported to the evaporator both through the MHPs' grooves and arteries. Soon afterward, the same group [39] stated that implanted arteries can effectively enhance the capillarity thus improving the capability to transport the liquid from the cold end back to the hot end, and limiting the propagation of dry-out region.

In addition to the artery MHPs, micro-grooves with non-parallel cross section were also utilized to enhance capillary effect and then heat transport capability of MHPs by Luo et al. [40]. A silicon-glass MHP with non-parallel micro-channel structure was put forward, having larger dimension of grooves in the evaporator section in comparison with that in the condenser section. Besides, a vapor chamber was wet etched onto the Pyrex 7740 glass and then bonded with the channel-etched silicon wafer as illustrated in **Figure 10**. The depths of the micro-grooves and vapor chamber in the silicon wafer and Pyrex 7740 were about 160 and 200 μm, respectively. Experimental results show that the non-parallel micro-channels could enhance the capillarity of liquid back flow from the condenser to the evaporator of the MHP and then improve the thermal performance. Also, it reveals that the vapor chamber influenced the performance of the MHP and a suitable design could reduce the vapor flow resistance and hence enhancing the liquid back flow. The novel MHPs demonstrate 10.6 times higher in the maximum equivalent thermal conductivity than that of the pure silicon wafer.
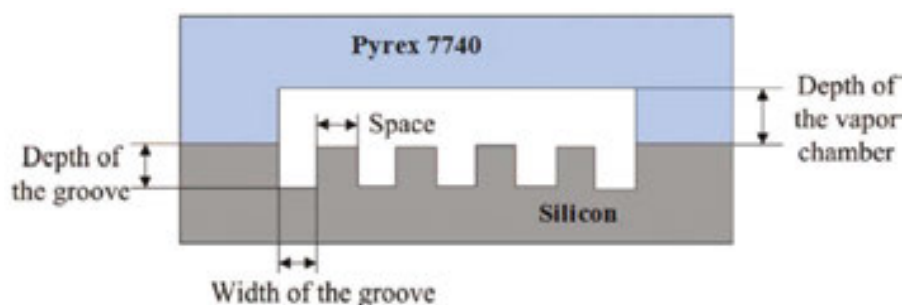

Figure 10. Schematic diagram of a micro-heat pipe with a vapor chamber [40].

In order to comprehensively understand the thermal performance of MHPs, micro-tempera-ture sensors including poly-silicon integrated thermistors [36, 41–44] and platinum resistance temperature detectors (RTDs) [45] were used to obtain temperature profile along the longitu-dinal axis of a MHP array precisely.

3.2. Theoretical analysis

While some analytical models that predict the heat transfer limitations and operating charac-teristics of individual MHPs have been developed [46–49], it is unclear how the incorporation of an array of these MHPs on a silicon wafer might affect the temperature distribution and the resulting thermal performance. Hence, Mallik et al. [31] developed a three-dimensional numerical model capable of predicting the thermal performance of an array of parallel MHPs constructed as an integral part of semiconductor chips. In order to determine the potential advantages of this concept, several different thermal loading configurations were analyzed. The reduction in maximum chip temperature, localized heat fluxes, and maximum tempera-

ture gradient across the chip as a function of the number of MHPs in the array was determined. Besides, the 3D numerical model was further extended to determine transient response characteristics of an array of MHPs integrated on silicon wafers. Numerical results show significant reductions in the transient response time, indicating the effectiveness of an array of these MHPs in dissipating heat over the entire chip surface and improving the heat removal capability. The transient thermal response was measured and compared with the calculations based on the numerical model proposed by the same group [33].

Suman and Kumar [50] and Suman and Hoda [51, 52] developed several one-dimensional models, which include the substrate effect, to predict the thermal characteristics of MHPs embedded in a silicon chip. These models are considerable simpler in form and easier to implement than those developed by other, while less accurate since only the fluid phase were took into account and neglected the liquid–vapor interface shear effect.

3.3. Novel designs for performance improvement

According to the working principles of a MHP, the liquid back flow is derived from a difference in the radius of curvature between the hot part and the cold part. Therefore, its heat transfer capacity is less than that of a conventional heat pipe having wicking structures. Owning to its advantages of simple design and direct integration on the silicon wafers, suitable for many applications, several attempts have been made in the past to increase the transport capability of MHPs.

By applying electric field at the liquid–vapor interface, pressure difference can be increased if the working fluid is dielectric in nature. This research is based on the assumption that both augmentation of the heat transport capability and active thermal control of MHPs can be achieved through the application of a static electric field. Yu et al. [53] conducted experimental and theoretical analyses to evaluate the potential benefits of electrohydrodynamic (EHD) forces on the operation of MHPs. In their experiments, the electric fields were used to orient and guide the flow of the dielectric liquid within the MHP from the condenser to the evaporator, and then a six time increase in the heat transport capability was obtained. The application of an electric field to MHPs not only can enhance the heat transfer capacity but also permits active thermal control of sources subject to transient heat loads and thus making the temperature control more precise [54].

Using EHD-assisted MHPs, the substrate temperature can be controlled more precise by varying the field strength. But the model developed by Yu et al. [53, 54] are semi-empirical in nature. The effect of electrical field has not been directly incorporated into flow of fluid. Therefore, a model developed from the first principle and its experimental validation is required to understand the effect of an electrical field in the performance of MHPs. Such an attempt has been presented by Suman [55] that developed a model for the fluid flow and heat transfer in an EHD-assisted MHP considering the coulomb and dielectrophoretic forces. The analytical expressions for the critical heat input and for the dry-out length have been obtained. It was found that the critical heat input could be increased by 100 times using EHD.

To provide enough capillary pressure to collect more working fluid at the evaporator region passively and enlarge the capillary limitation, surface wettability treatment of inner wall along the longitudinal direction of a MHP offers a possible solution. Qu et al. [56] proposed a triangular MHP characterized by a gradient inner surface, with the evaporator, adiabatic section, and condenser having different surface wettabilities and hence contact angles. The contact angle decreases from the condenser to the evaporator, thereby enhancing heat transfer capacity. The results revealed that the surface with a gradient wettability increased the maximum heat input of the MHP up to 49.7%, compared with that of uniform surface wettability. The effect of surface-tension gradient on the thermal performance of a MHP has been numerically investigated by Suman [57]. Results show that the liquid pressure drop across the MHP can be decreased by about 90%, and the maximum heat throughput can be increased by about 20% with a favorable surface-tension gradient. A mixture of water and normal alcohol with carbon chain ranging 4–7 (like water-butanol mixture) was suggested to
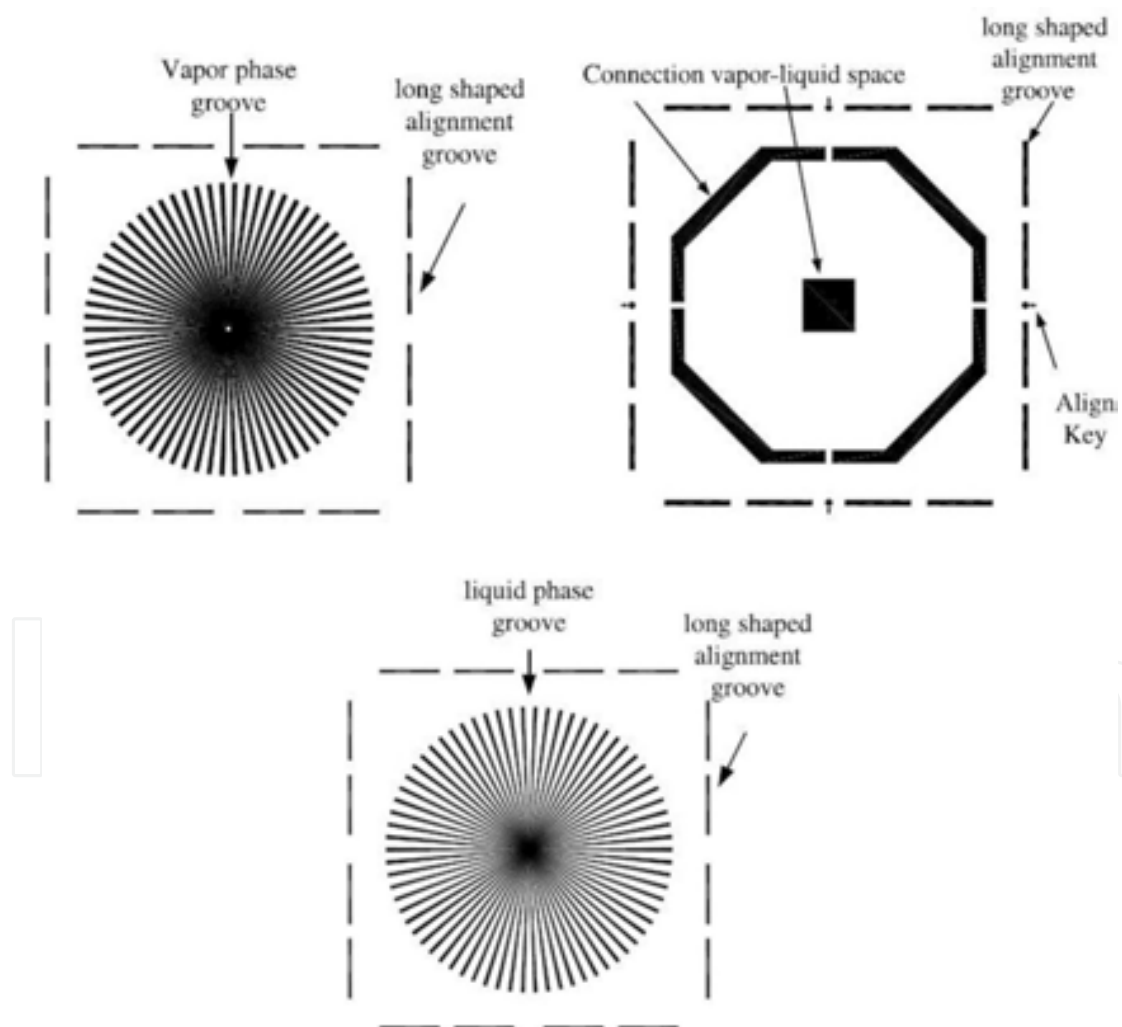

Figure 11. A radial-grooved micro-heat pipe: vapor-phase grooves (top left); interface (top right); liquid phase grooves (bottom) [58].

use as a liquid solution whose surface tension increases with the increase of temperature. The favorable effects will promote the fluid flow from the cold end to the hot end resulting in the heat transfer enhancement of a MHP.

A radial-grooved MHP as illustrated in **Figure 11** was designed and fabricated in silicon wafer by Kang et al. [58]. This radial-grooved MHP consisted of a three-layer structure, with the middle layer serving as the interface between liquid and vapor phases flowing in the upper and bottom layers, respectively. The separation of the liquid and vapor flow was designed to reduce the viscous shear force. This MHP with a size of 5 cm × 5 cm was fabricated by bulk micro-machining and eutectic bonding techniques. Both the vapor and liquid phase grooves were 23 mm in length and trapezoidal in shape, with 70 grooves spreading in a radial manner from the center outward. For the vapor phase grooves, the widths at the inner and outer ends of the grooves were 350 and 700 μm, respectively. The corresponding widths for the liquid phase grooves at inner and outer end are 150 and 500 μm, respectively. The best heat transfer performance of 27 W at a filling rate of 70% was obtained for this micro-device. Later, Kang et al. [59] presented two wick designs of MHPs with three copper foil layers. The first design has almost the same structures as depicted in **Figure 11** and worked based on the same principle and advantages of liquid–vapor separation, whereas the second one had 100-mesh copper screens as wicking structure (**Figure 12**). It was found that the radial grooved MHP, filled with methanol at a filling ratio of 82%, showed better performance at a heat input of 35 W than that using mesh screens as wicking structure.
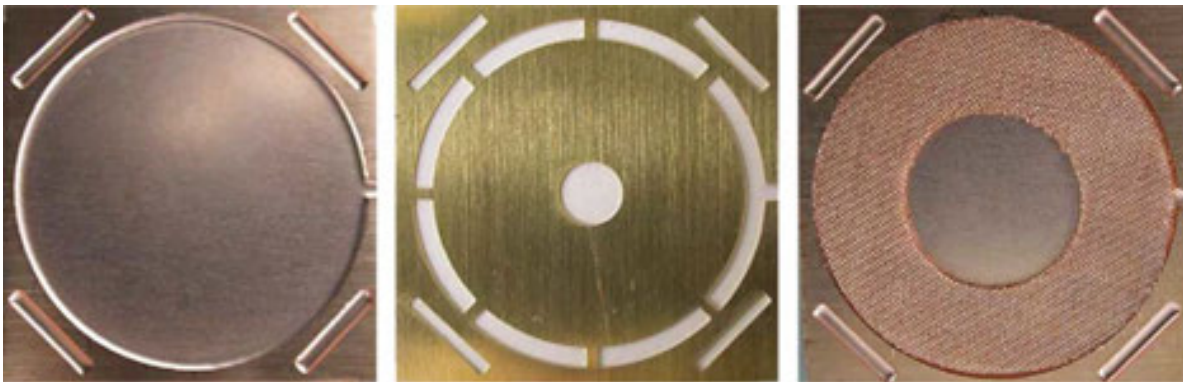
Figure 12. The diagram about the structures of each layer of a copper-screen-styled micro-heat pipe heat spreader: gas phase (left); partition panel (central); liquid phase (right) [59].

4. Other emerging MEMS-based MHPs

In addition to MEMS-based micro-grooved heat pipes, some other mini- or micro-scale heat pipes, such as capillary pumped loops (CPLs) [60–64], loop heat pipes (LHPs) [65–69], oscillating heat pipes (OHPs) [70–75], and vapor chambers (VCs) [76–80] as shown **Figure 13**, were also successfully constructed on silicon substrates by means of micro-fabrication technique recent years and became two-phase passive micro-coolers for electronic cooling.

Figure 13. Novel MEMS-based micro-heat pipes: (a) micro-CPL [62], (b) micro-LHP [65], (c) micro-OHP [72], and (d) micro-vapor chamber [77].

Similar to MEMS-based micro-grooved heat pipes, these novel MEMS-based MHPs could be considered as small versions of corresponding conventional prototypes and work at the related mechanism. Although some of these micro-devices have more complicated structures in comparison with micro-grooved heat pipes, especially the micro-CPLs and micro-LHP consisting of additional wicking structures, the heat cooling capability is much higher and the maximum allowable heat fluxes could be up to 185.2 W/cm^2 [63] and 300 W/cm^2 [68] for micro-CPLs and micro-LHP, respectively.

In addition to MEMS-based loop-type heat pipes as shown in Figure 13a–c, MEMS-based VCs are also utilized for spreading high local heat flux and act as silicon heat spreaders. A silicon VC illustrated in **Figure 13**d based on a unique three-layer silicon wafer-stacking fabrication process demonstrated an maximum effective thermal conductivity about 2700 W/(m K) [77], indicating excellent performance to attain temperature uniformity.

To further increase the heat transport capability of micro-VCs, recently micro-/nano-hierarchical wicking structures are proposed by researches. The materials of carbon nanotube, Ti, and Cu as shown in Figure 14 are available due to the easy-fabrication feasibility and material compatibility. As compared to the micro-wicking structures, the micro-/nano-biwick structure

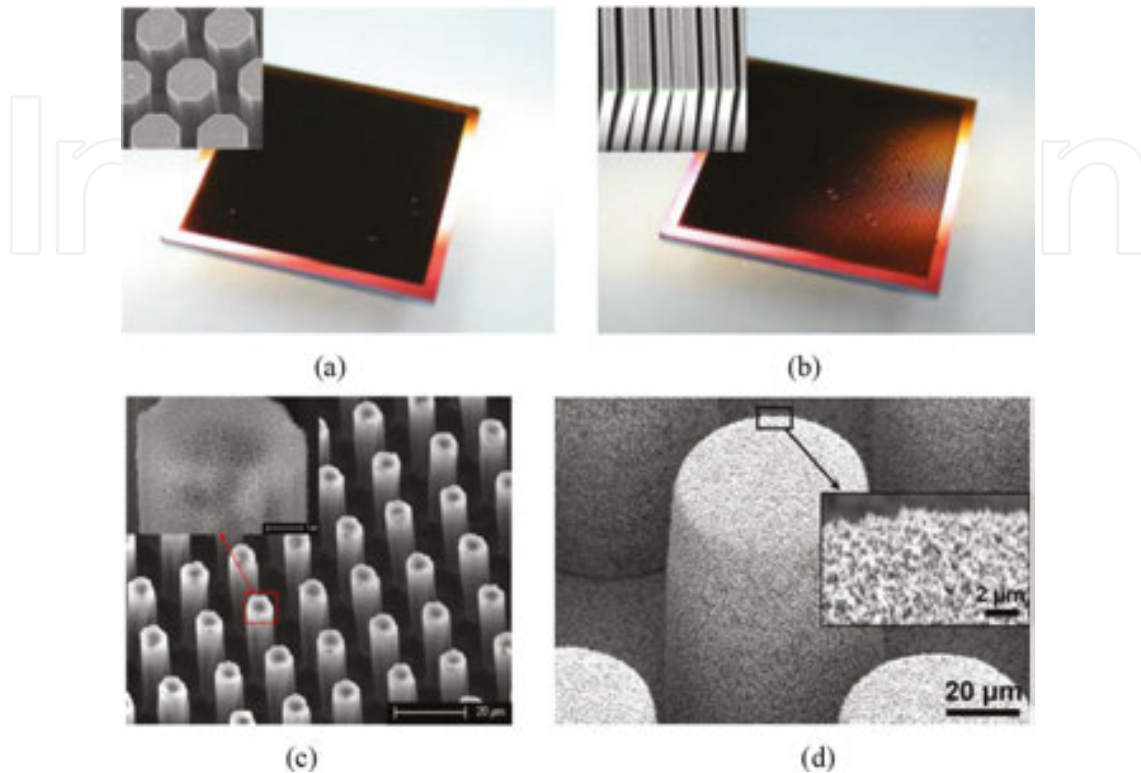shows better wettability [82, 83] and can sustain ultra-high localized heat flux over 700 W/cm² [81].

Figure 14. SEM images of micro-/nano-hierarchical wicking structures for micro-vapor chamber: (a) biwick structure composed of cylindrical CNT pillars [81]; (b) biwick structure composed of straight CNT stripes [81]; (c) Ti pillar array with oxidized hairlike NST(nanostructured titania) [82]; (d) nanostructured Cu micro-posts [83].

5. Applications of MEMS-based MHPs

The most ongoing and potential application of MEMS-based MHPs is in the thermal management of electronics [84, 85]. Adkins et al. [86] discussed the use of a "heat-pipe heat spreader" embedded in a silicon substrate as an alternative to the conductive cooling of integrated circuits using diamond films. These MHPs function as highly efficient heat spreaders, collecting heat from the localized hot spots and dissipating the heat over the entire chip surface. Incorporation of these MHPs as an integral part of silicon wafers has been shown to significantly reduce the maximum wafer temperature and reduce the temperature gradients occurring across these devices [28, 32]. Currently, mobile electronics, such as smart phones and tablet PCs, are widely used and becoming an alternate solution of traditional PCs or notebooks. These devices comprise many high-heat-generating components and have been miniaturized and designed for high-density packaging. The complex thermal behavior due to their usage under various circumstances affects the reliability and usability. The ultra-compact cooling space demands

of these mobile electronics make the MEMS-based MHPs a good alternative solution as compared to other cooling schemes.

The biological field associated with human disease remedy is another potential application of MEMS-based MHPs. MHPs can provide a controllable heat rate at constant temperature and may be matched to the thermal conductivity of live tissue and the degree to which a cancerous tumor is perfused. They may be useful in treating cancerous tumors in body regions that cannot be treated by other means [87, 88].

In addition to the above applications, the thermal management of localized heat generating devices such as concentrated solar cells, MEMS-based infrared detectors and micro-fuel cells as well as thermal energy harvesting devices is also possible fields that MEMS-based MHPs can be used.

6. Summary

In this chapter, a generalized concept of MEMS-based MHPs is proposed on the basis of the initial description of MHP by Cotter as an integral part of semiconductor devices. The working principle, capillary limitation, fabrication process as well as the state-of-the-art of MEMS-based micro-grooved heat pipes have been introduced firstly and discussed in detail. Some new MEMS-based MHPs, including micro-CPLs, micro-LHPs, micro-OHPs, and micro-VCs, and some of their structures and thermal characteristics have been presented. In view of the continued trend in miniaturization of electronic/optoelectronic devices and circuits and explosive growth of MEMS products, MEMS-based MHPs exhibit advantages and will find increasing applications in related engineering and medical fields. More research work is needed to provide rational tools for optimal designs and fabrications of these micro-devices.

Acknowledgements

Nomenclature

A	Cross-sectional area (m²)
Bo	Bond number
C	Constant
f	Fanning friction factor
g	Gravitational acceleration (m s⁻²)
h_{fg}	Vaporization latent heat (J kg⁻¹)

K	Permeability (m^2)
L	Length (m)
Ma	Mach number
Δp	Pressure difference (Pa)
Q	Heat transfer rate (W)
r	Radius of curvature (m)

Greek symbols

μ	Dynamic viscosity (kg m^{-1}s^{-1})
ρ	Density (kg m^{-3})
σ	Surface tension (N m^{-1})

Subscripts

a	Adiabatic section
c	Condenser section, capillary radius
e	Evaporator section
eff	Effective
g	Gas
h	Hydraulic radius
l	Liquid
v	Vapor

Author details

Qu Jian* and Wang Qian

*Address all correspondence to: rjqu@mail.ujs.edu.cn

School of Energy and Power Engineering, Jiangsu University, Zhenjiang, China

References

[1] He YL, Tao WQ. Convective heat transfer enhancement: Mechanisms, techniques, and performance evaluation. Advances in Heat Transfer. 2014; 46: 88–186.

[2] Agostini B, Fabbri M, Park JE, Wojtan L, Thome JR, Michel B. State of the art of high heat flux cooling technologies. Heat Transfer Engineering. 2007; 28(4): 258–281.

[3]   Garimella SV, Fleischer AS, Murthy JY, Keshavarzi A, Prasher R, Patel C, Bhavnani SH, Venkatasubramanian R, Mahajan R, Joshi Y, Sammakia B, Myers BA, Chorosinski L, Baelmans M, Sathyamurthy P, Raad PE. Thermal challenges in next-generation electronic systems. IEEE Transactions on Components and Packaging Technologies. 2008; 31(4): 801–815.

[4]   Ebadian MA, Lin CX. A review of high-heat-flux heat removal technologies. Journal of Heat Transfer. 2011; 133(11): 110801.

[5]   Marcinichen JB, Olivier JA, Lamaison N, Thome JR. Advances in electronics cooling. Heat Transfer Engineering. 2013; 34(5–6): 434–446.

[6]   Cotter TP. Principles and prospects of micro-heat pipes. Proceedings of the 5th International Heat Pipe Conference. 1984.

[7]   Suman B. Microgrooved heat pipe. Advanced in Heat Transfer. 2009; 41: 1–80.

[8]   Babin BR, Peterson GP, Wu D. Steady-state modeling and testing of a micro heat pipe. Journal of Heat Transfer. 1990; 112(3): 595–601.

[9]   Cao Y, Faghri A. Micro/miniature heat pipes and operating limitations. Journal of Enhanced Heat Transfer. 1994; 1(3): 265–274.

[10] Zaghdoudi MC, Maalej S, Mansouri J, Sassi MBH. Flat miniature heat pipes for electronics cooling: state of the art, experimental and theoretical analysis. International Journal of Engineering and Applied Sciences. 2011; 7(3): 166–189.

[11] Cao Y, Faghri A, Mahefkey ET. Micro/Miniature Heat Pipes and Operating Limitations. ASME-PUBLICATIONS-HTD. 1993.

[12] Mohamed GH. The MEMS Handbook. Boca Raton: CRC. 2002.

[13] Gerner FM, Longtin JP, Henderson HT, Hsieh WM, Ramadas P, Chang WS. Flow and heat transfer limitations in micro heat pipes. ASME, HTD-Vol. 206-3, 1992, San Diego, CA, USA.

[14] Peterson GP. Modeling, fabrication, and testing of micro heat pipes: An update. Applied Mechanics Reviews. 1996; 49: S175–83.

[15] Sobhan CB, Rag RL, Peterson GP. A review and comparative study of the investigations on micro heat pipe. International Journal of Energy Research. 2007; 31: 664–688.

[16] Suman B. Modeling, experiment, and fabrication of micro-grooved heat pipes: An update. Applied Mechanics Reviews. 2007; 60(3): 107–119.

[17] Peterson GP. An Introduction to Heat Pipes: Modeling, Testing and Applications. New York: John Wiley & Sons, INC. 1994.

[18] Faghri A. Review and advances in heat pipe science and technology. Journal of Heat Transfer. 2012; 134(12): 123001.

[19] Chakraborty S. Microfluidics and Microscale Transport Processes. Boca Raton: CRC Press, Taylor & Francis Group. 2012.

[20] Faghri A. Performance characteristics of a concentric annular heat pipe part II: Vapor flow analysis. Journal of Heat Transfer. 1989; 111(4): 851–857.

[21] Kim BH, Peterson GP. Analysis of the critical Weber number at the onset of liquid entrainment in capillary-driven heat pipes. International Journal of Heat and Mass Transfer. 1995; 38(8): 1427–1442.

[22] Suman B, De S, DasGupta S. A model of the capillary limit of a micro heat pipe and prediction of the dry-out length. International Journal of Heat and Fluid Flow. 2005; 26(3): 495–505.

[23] Shukla KN. Heat transfer limitation of a micro heat pipe. Journal of Electronic Packaging. 2009; 131(2): 024502.

[24] Zohar Y. Heat convection in micro ducts. Springer Science & Business Media, Netherlands, 2013.

[25] Ma HB. Micro heat pipes. Encyclopedia of Microfluidics and Nanofluidics. 2015; 1813–1825.

[26] Peterson GP, Duncan AB, Ahmed AS, Mallik AK, Weichold MH. Experimental investigation of micro heat pipes in silicon wafers. Winter Annual Meeting of the American Society of Mechanical Engineers. 1991.

[27] Gerner FM. Micro Heat Pipes. AFSOR Final Report No. S-210-10MG-066. 1990.

[28] Peterson GP, Duncan AB, Weichold MH. Experimental investigation of micro heat pipes fabricated in silicon wafers. Journal of Heat Transfer. 1993; 115(3): 751–756.

[29] Laermer F, Urban A. Challenges, developments and applications of silicon deep reactive ion etching. Microelectronic Engineering. 2003; 67: 349–355.

[30] Marty F, Rousseau L, Saadany B, Mercier B, Français O, Mita Y, Bourouina T. Advanced etching of silicon based on deep reactive ion etching for silicon high aspect ratio microstructures and three-dimensional micro-and nanostructures. Microelectronics Journal. 2005; 36(7): 673–677.

[31] Mallik AK, Peterson GP, Weichold MH. On the use of micro heat pipes as an integral part of semiconductor devices. Journal of Electronic Packaging. 1992; 114(4): 436–442.

[32] Weichold MH, Peterson GP, Mallik A. Vapor deposited micro heat pipes. US Patent 5, 1993.

[33] Peterson GP, Mallik AK. Transient response characteristics of vapor deposited micro heat pipe arrays. Journal of Electronic Packaging. 1995; 117(1): 82–87.

[34] Mallik AK, Peterson GP. Steady-state investigation of vapor deposited micro heat pipe arrays. Journal of Electronic Packaging. 1995; 117(1): 75–81.

[35] Badran B, Gerner FM, Ramadas P, Henderson T, Baker KW. Experimental results for low-temperature silicon micromachined micro heat pipe arrays using water and methanol as working fluids. Experiment Heat Transfer. 1997; 10: 253–272.

[36] Berre ML, Launay S, Sartre V, Lallemand M. Fabrication and experimental investigation of silicon micro heat pipes for cooling electronics. Journal of Micromechanics and Microengineering. 2003; 13(3): 436.

[37] Kang SW, Huang D. Fabrication of star grooves and rhombus grooves micro heat pipe. Journal of Micromechanics and Microengineering. 2002; 12(5): 525.

[38] Kang J, Fu X, Liu W, Dario P. Investigation on Microheat Pipe Array with Arteries. Journal of Thermophysics and Heat Transfer. 2010; 24(4): 803–810.

[39] Liu W, Kang J, Fu X, Stefanini C, Dario P. Analysis on heat resistance of the micro heat pipe with arteries. Microelectronic Engineering. 2011; 88(8): 2255–2258.

[40] Luo Y, Liu G, Zou LL, Yu BK, Wang XD. Thermal behavior investigation of silicon-Pyrex micro heat pipe. AIP Advances. 2014; 4(3): 031305.

[41] Lee M, Wong M, Zohar Y. Characterization of an integrated micro heat pipe. Journal of Micromechanics and Microengineering. 2003; 13(1): 58.

[42] Launay S, Sartre V, Lallemand M. Experimental study on silicon micro-heat pipe arrays. Applied Thermal Engineering. 2004; 24(2): 233–243.

[43] Berre ML, Pandraud G, Morfouli P, Lallemand M. The performance of micro heat pipes measured by integrated sensors. Journal of Micromechanics and Microengineering. 2006; 16(5): 1047.

[44] Lee M, Wong M, Zohar Y. Integrated micro-heat-pipe fabrication technology. Journal of Microelectromechanical Systems. 2003; 12(2): 138–146.

[45] Harris DK, Palkar A, Wonacott G, Dean R, Simionescu F. An experimental investigation in the performance of water-filled silicon microheat pipe arrays. Journal of Electronic Packaging. 2010; 132(2): 021005.

[46] Babin BR, Peterson GP, Wu D. Steady-state modeling and testing of a micro heat pipe. Journal of Heat Transfer. 1990; 112(3): 595–601.

[47] Longtin JP, Badran B, Gerner FM. A one-dimensional model of a micro heat pipe during steady-state operation. Journal of Heat Transfer. 1994; 116(3): 709–715.

[48] Khrustalev D, Faghri A. Thermal analysis of a micro heat pipe. Journal of Heat Transfer. 1994; 116(1): 189–198.

[49] Peterson GP, Ma HB. Theoretical analysis of the maximum heat transport in triangular grooves: A study of idealized micro heat pipes. Journal of Heat Transfer. 1996; 118(3): 731–739.

[50] Suman B, Kumar P. An analytical model for fluid flow and heat transfer in a micro-heat pipe of polygonal shape. International Journal of Heat and Mass Transfer. 2005; 48(21–22): 4498–4509.

[51] Suman B, Hoda N. Effect of variations in thermophysical properties and design parameters on the performance of a V-shaped micro grooved heat pipe. International Journal of Heat and Mass Transfer. 2005; 48(10): 2090–2101.

[52] Suman B, Hoda N. On the transient analysis of a V-shaped microgrooved heat pipe. Journal of Heat Transfer. 2007; 129(11): 1584–1591.

[53] Yu Z, Hallinani K, Bhagat W, Kashani RA. Electrohydrodynamically augmented micro heat pipes. Journal of Thermophysics and Heat Transfer. 2002; 16(2): 180–186.

[54] Yu Z, Hallinan K P, Kashani RA. Temperature control of electrohydrodynamic micro heat pipes. Experimental Thermal and Fluid Science. 2003; 27(8): 867–875.

[55] Suman B. A steady state model and maximum heat transport capacity of an electrohydrodynamically augmented micro-grooved heat pipe. International Journal of Heat and Mass Transfer. 2006; 49(21): 3957–3967.

[56] Qu J, Wu H, Cheng P. Effects of functional surface on performance of a micro heat pipe. International Communications in Heat and Mass Transfer. 2008; 35(5): 523–528.

[57] Suman B. Effects of a surface-tension gradient on the performance of a micro-grooved heat pipe: an analytical study. Microfluidics and Nanofluidics. 2008; 5(5): 655–667.

[58] Kang SW, Tsai SH, Chen HC. Fabrication and test of radial grooved micro heat pipes. Applied Thermal Engineering. 2002; 22(14): 1559–1568.

[59] Kang SW, Tsai SH, Ko MH. Metallic micro heat pipe heat spreader fabrication. Applied Thermal Engineering. 2004; 24(2): 299–309.

[60] Kirshberg J, Yerkes K, Liepmann D. Micro-cooler for chip-level temperature control. SAE Aerospace Power Systems Conference. 1999.

[61] Kirshberg J, Yerkes K, Trebotich D, Liepmann D. Cooling effect of a MEMS based micro capillary pumped loop for chip-level temperature control. ASME MEMS. 2000.

[62] Liepmann D. Design and fabrication of a micro-CPL for chip-level cooling. Proceedings of ASME International Mechanical Engineering Congress and Exposition. 2001.

[63] Wang CT, Leu TS, Lai TM. Micro capillary pumped loop system for a cooling high power device. Experimental Thermal and Fluid Science. 2008; 32(5): 1090–1095.

[64] Moon SH, Hwang G. Development of the micro capillary pumped loop for electronic cooling. THERMINIC. 2007.

[65] Hsu C, Kang S, Hou T. Performance testing of micro loop heat pipes. Tamkang Journal of Science and Engineering. 2005; 8: 123–32.

[66] Cytrynowicz D, Hamdan M, Medis P, Shuja A, Henderson HT, Gerner FM, Golliher E. MEMS Loop Heat Pipe Based on Coherent Porous Silicon Technology. Proceedings of Space Technology and Applications International Forum. 2002.

[67] Cytrynowicz D, Medis P, Parimi S, Shuja A, Henderson HT, Gerner FM. The MEMS loop heat pipe based on coherent porous silicon-The modified system test structure. AIP Conference Proceedings. 2004.

[68] Ghajar M, Darabi J, and Jr NC. A hybrid CFD-mathematical model for simulation of a MEMS loop heat pipe for electronics cooling applications. Journal of Micromechanics and Microengineering. 2005; 15(2): 313–321.

[69] Ghajar M, Darabi J. Evaporative heat transfer analysis of a micro loop heat pipe with rectangular grooves. International Journal of Thermal Sciences. 2014; 79: 51–59.

[70] Qu J, Wu H Y. Flow visualization of silicon-based micro pulsating heat pipes. Science China Technological Sciences. 2010; 53(4): 984–990.

[71] Qu J, Wu H, Wang Q. Experimental investigation of silicon-based micro-pulsating heat pipe for cooling electronics. Nanoscale and Microscale Thermophysical Engineering. 2012; 16(1): 37–49.

[72] Qu J, Wu H, Cheng P. Start-up, heat transfer and flow characteristics of silicon-based micro pulsating heat pipes. International Journal of Heat and Mass Transfer. 2012; 55(21): 6109–6120.

[73] Youn YJ, Kim SJ. Fabrication and evaluation of a silicon-based micro pulsating heat spreader. Sensors and Actuators A: Physical. 2012; 174: 189–197.

[74] Yang KS, Cheng YC, Liu MC, Shyu JC. Micro pulsating heat pipes with alternate microchannel widths. Applied Thermal Engineering. 2015; 83: 131–138.

[75] Kwon GH, Kim SJ. Experimental investigation on the thermal performance of a micro pulsating heat pipe with a dual-diameter channel. International Journal of Heat and Mass Transfer. 2015; 89: 817–828.

[76] Cai Q, Chen BC, Tsai C, Chen CL. Development of scalable silicon heat spreader for high power electronic devices. Journal of Thermal Science and Engineering Applications. 2009; 1(4): 041009.

[77] Cai Q, Chen B, Tsai C. Design, development and tests of high-performance silicon vapor chamber. Journal of Micromechanics and Microengineering. 2012; 22(3): 035009.

[78] Cai Q, Bhunia A, Tsai C, Kendig MW. DeNatale JF. Studies of material and process compatibility in developing compact silicon vapor chambers. Journal of Micromechanics and Microengineering. 2013; 23(6): 065003.

[79] Wei M, Somasundaram S, He B, Liang Q, Tan CS, Wang EN. Experimental characterization of Si micropillar based evaporator for advanced vapor chambers. IEEE 16th Electronics Packaging Technology Conference. 2014.

[80] Yang KS, Lin CC, Shyu JC, Tsenga CY, Wang CC. Performance and two-phase flow pattern for micro flat heat pipes. International Journal of Heat and Mass Transfer. 2014; 77: 1115–1123.

[81] Cai Q, Chen YC. Investigations of biporous wick structure dryout. Journal of Heat Transfer. 2012; 134(2): 021503.

[82] Ding C, Soni G, Bozorgi P, Piorek BD, Meinhart CD, MacDonald NC. A flat heat pipe architecture based on nanostructured titania. Journal of Microelectromechanical Systems. 2010; 19(4): 878–884.

[83] Nam Y, Ju YS. A comparative study of the morphology and wetting characteristics of micro/nanostructured Cu surfaces for phase change heat transfer applications. Journal of Adhesion Science and Technology. 2013; 27(20): 2163–2176.

[84] Vasiliev LL. Micro and miniature heat pipes–electronic component coolers. Applied Thermal Engineering. 2008; 28(4): 266–273.

[85] Chen X, Ye H, Fan X, Ren T, Zhang G. A review of small heat pipes for electronics. Applied Thermal Engineering. 2016; 96: 1–17.

[86] Adkins DR, Shen DS, Palmer DW, Tuck MR. Silicon heat pipes for cooling electronics. Sandia National Labs., Albuquerque, NM (United States), 1994.

[87] Fletcher LS, Peterson GP. Micro-heat-pipe catheter: US Patent 5, 1993.

[88] Fletcher LS, Peterson GP. Method of treating diseased tissue: US Patent 5, 1997.